

## Electronic Supplementary Information

# Unravelling the role of nanoparticle morphology during uptake and transport in eggplants†

Lifei Xi,<sup>a, b</sup> Yamin Wang,<sup>b</sup> Alfiz Muhammad Qizwini,<sup>b</sup> Yee Yan Tay,<sup>a</sup> Chris Boothroyd<sup>a, b</sup> and Yeng Ming Lam<sup>\*, a, b</sup>

<sup>a</sup>Facility for Analysis, Characterisation, Testing and Simulation (FACTS), Nanyang Technological University, Singapore 639798

<sup>b</sup>School of Materials Science and Engineering, Nanyang Technological University, Singapore 639798

## Supplementary table and figures

### 1. Supplementary table

**Table S1.** Summary of main IR frequencies with assignments of Au nanocarriers and a few initial chemicals obtained from this study.

Wavenumber (cm <sup>-1</sup> )							Assignment
β-CD	Au nanospheres	Au nanowires	Cu-EDTA	RhB	Au spherical nanocarriers	Au wire nanocarriers	
3543	3543				3543		–OH stretching <sup>1</sup>
		3431	3426		3423	3436	OH groups and physically absorbed water <sup>2</sup>
3329	3316				3316		–OH stretching <sup>3,4,5,6</sup>
2938	2934	2941	2931		2942	2949	aliphatic C–H stretches <sup>7</sup>
2885	2885	2885			2887	2893	CH <sub>2</sub> bending <sup>8,1</sup>
				1705	1705	1705	Carbonyl stretch, ν(C=O) of the ester group of RhB <sup>9,10</sup>
1663	1660	1646			1660	1658	H–O–H deformation bands of water <sup>1</sup>
			1604		1606	1601	Asymmetry stretch, ν <sub>a</sub> (C=O) of the COO <sup>-</sup> group <sup>11</sup>
				1592	1592	1592	In-plane C=C skeletal stretching vibration <sup>9,10</sup>
1462	1462	1462		1467	1466	1463	–COO <sup>-</sup> <sup>12</sup>
1414	1414	1414		1411	1416	1409	–COO <sup>-</sup> <sup>12</sup>
			1391		1398	1402	Symmetry stretching, ν <sub>s</sub> (COO <sup>-</sup> ) <sup>11,2</sup>
			1326		1320	1320	Stretch, ν <sub>t</sub> (CH <sub>2</sub> ) <sup>11</sup>
				1275	1275	1261	C–N stretch
			1251	1248	1248	1250	C–H bending vibration <sup>13</sup>

					1219	1219	C-N stretch
			1182		1180	1185	O-H bending vibration <sup>13</sup>
1161	1162	1162		1162	1162	1162	C-O-C vibration <sup>1</sup> asymmetric glycosidic stretch, $\nu_a(\text{C-O-C})^{5, 6}$
			1133		1133	1133	C-H, C-O stretching <sup>1</sup>
			1117		1117	1108	C-N <sup>11</sup>
1084	1084	1081		1077	1077	1075	Coupled stretch vibration $\nu(\text{C-C/C-O})^{6, 5}$
1037	1037	1037			1044	1043	Coupled stretch vibration $\nu(\text{C-C/C-O})^5$
			928	923	923	920	-COO <sup>-12</sup>
861	861	861			868	872	Out-of- plane bending vibration $\nu(\text{C-H})^{6, 5}$
761	761	752			745	741	Ring 'breathing' vibration <sup>4,14</sup>
704	705	704			704	705	Pyranose ring vibration <sup>14</sup>

## 2. Supplementary figures

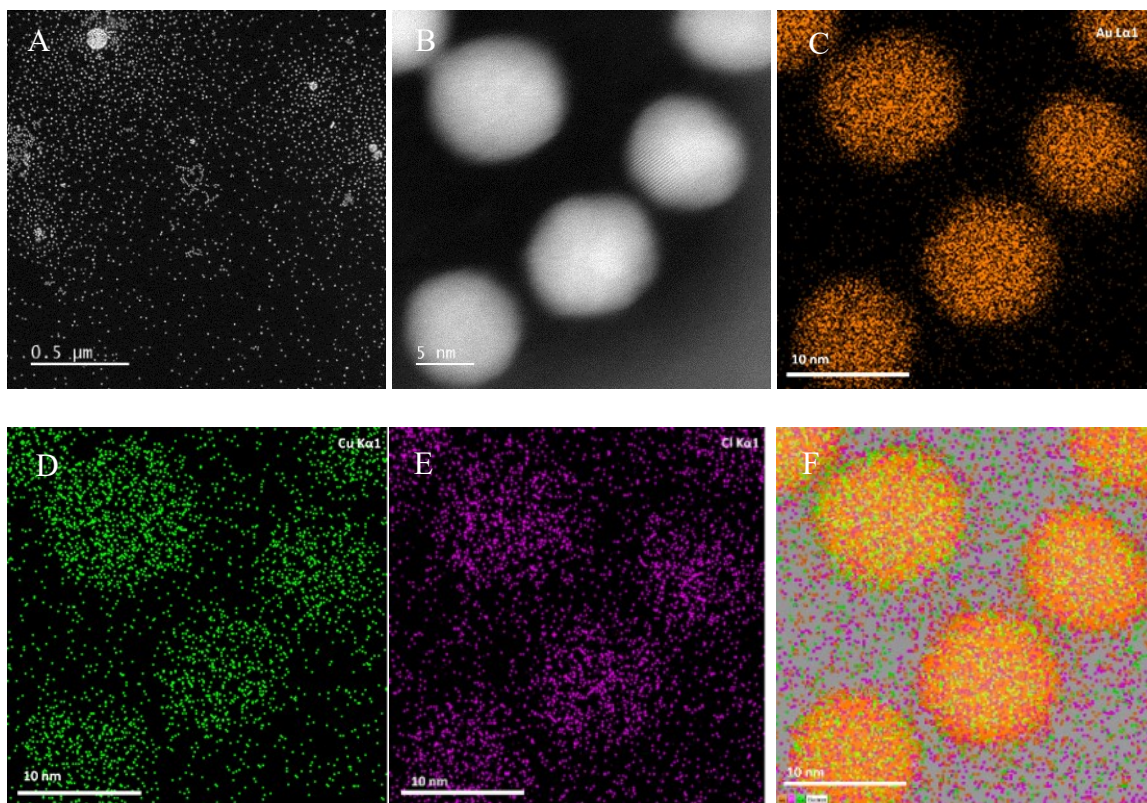


**Fig. S1** (A, B) Additional HAADF-STEM images of Au spherical nanocarriers. (C-F) EDX maps of (C) Au, (D) Cu, (E) Cl and (F) combined Au, Cu and Cl map of Au spherical nanocarriers.

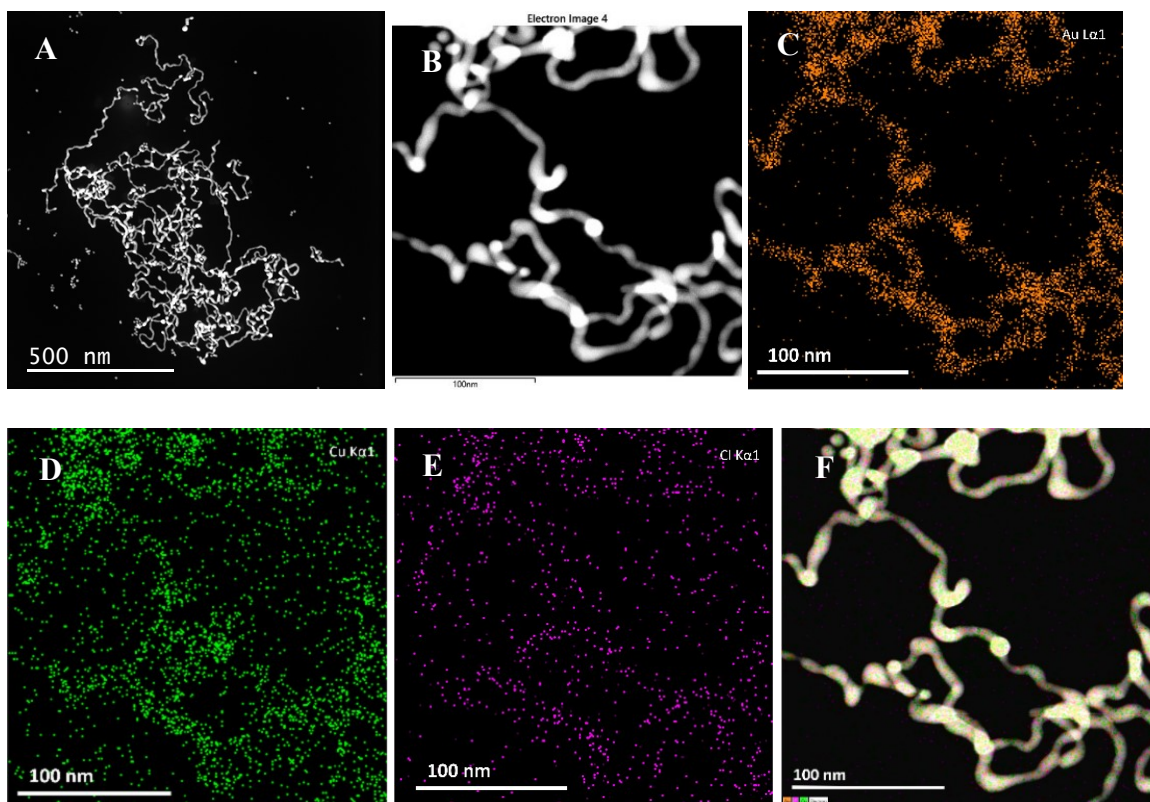


**Fig. S2** (A, B) Additional HAADF-STEM images of the Au wire nanocarriers. (C-F) EDX maps of (C) Au, (D) Cu, (E) Cl and (F) combined Au, Cu and Cl map of Au wire nanocarriers.

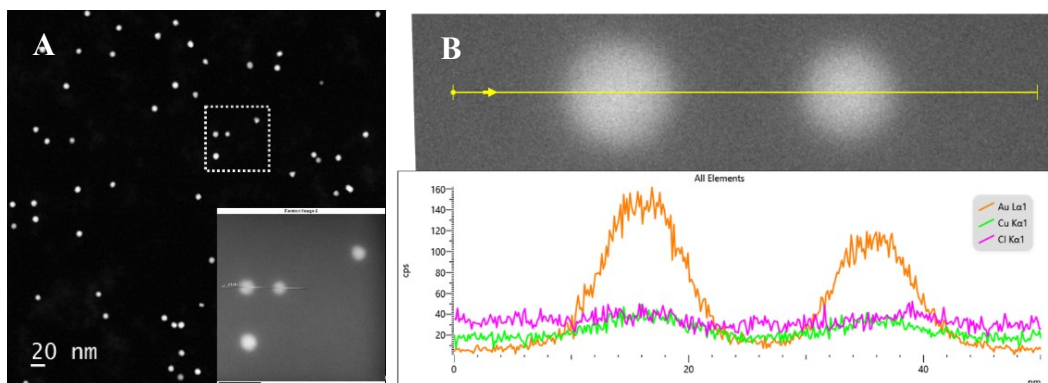


**Fig. S3** (A-B) HAADF-STEM images and EDX linescan profile of Au spherical nanocarriers. Note: the dotted box and inset image in (A) shows the location from where the linescan (B) was taken. The linescan profile in (B) clearly shows that the signal intensities of Cl and Cu are at the same level although sample and TEM grid contains no Cu at all.

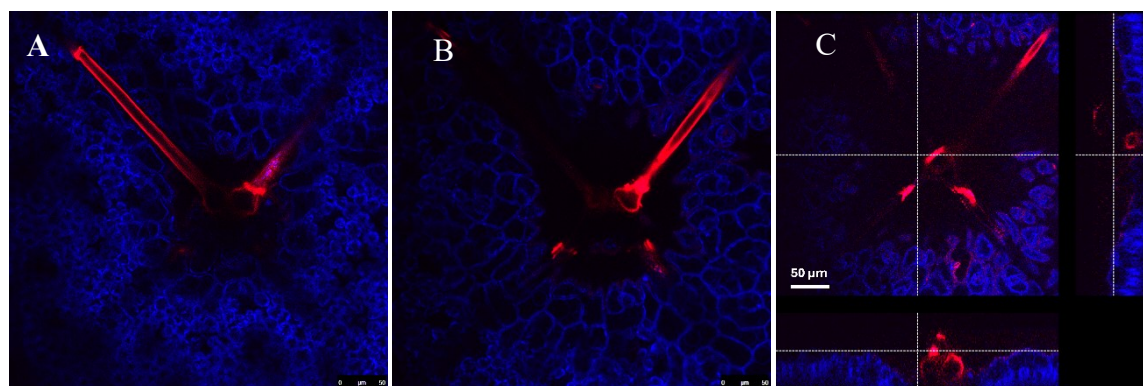


**Fig. S4** Confocal microscopy analysis showing the biodistribution of Rhodamine B-labelled Au spherical nanocarriers in the vein of an eggplant leaf. (A-B) Images at different Z-focus levels. The Rhodamine B (RhB) signal is depicted in red, and the autofluorescence from chlorophyll is shown in blue. (C) Z-stack scan from the leaf sample highlighting the vascular vein structure and localized nanocarrier distribution: z-stacks. The stack was acquired with a 1.0 µm z-step resolution across a total scanning depth of 58 µm.

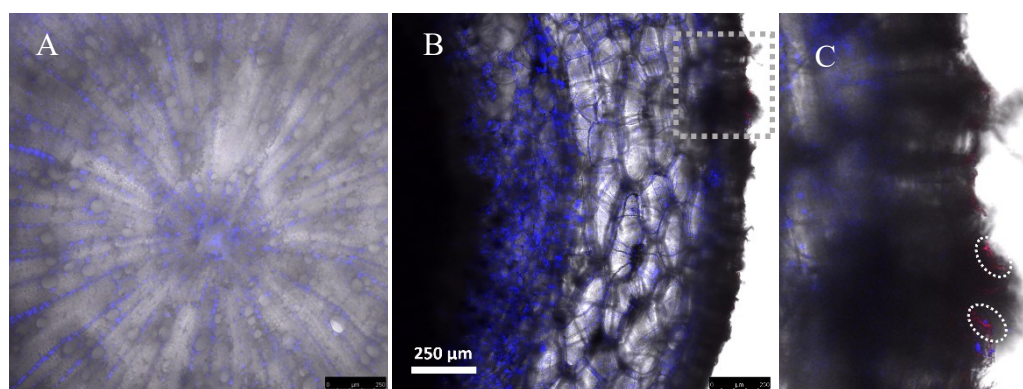


**Fig. S5** Additional confocal microscopy analysis of the biodistribution of rhodamine B labelled Au spherical nanocarriers in the stem of an eggplant. (A) Image showing overview of the stem. (B) A region containing a rhodamine B signal. (C) Enlarged image of the area marked in (B).

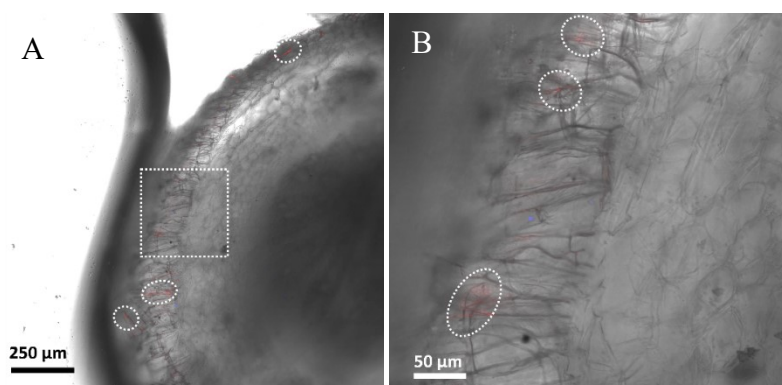


**Fig. S6** Confocal microscopy analysis of the biodistribution of rhodamine labelled Au spherical nanocarriers in the root of an eggplant.

(B) Enlarged image of the area marked with a dotted square in (A).

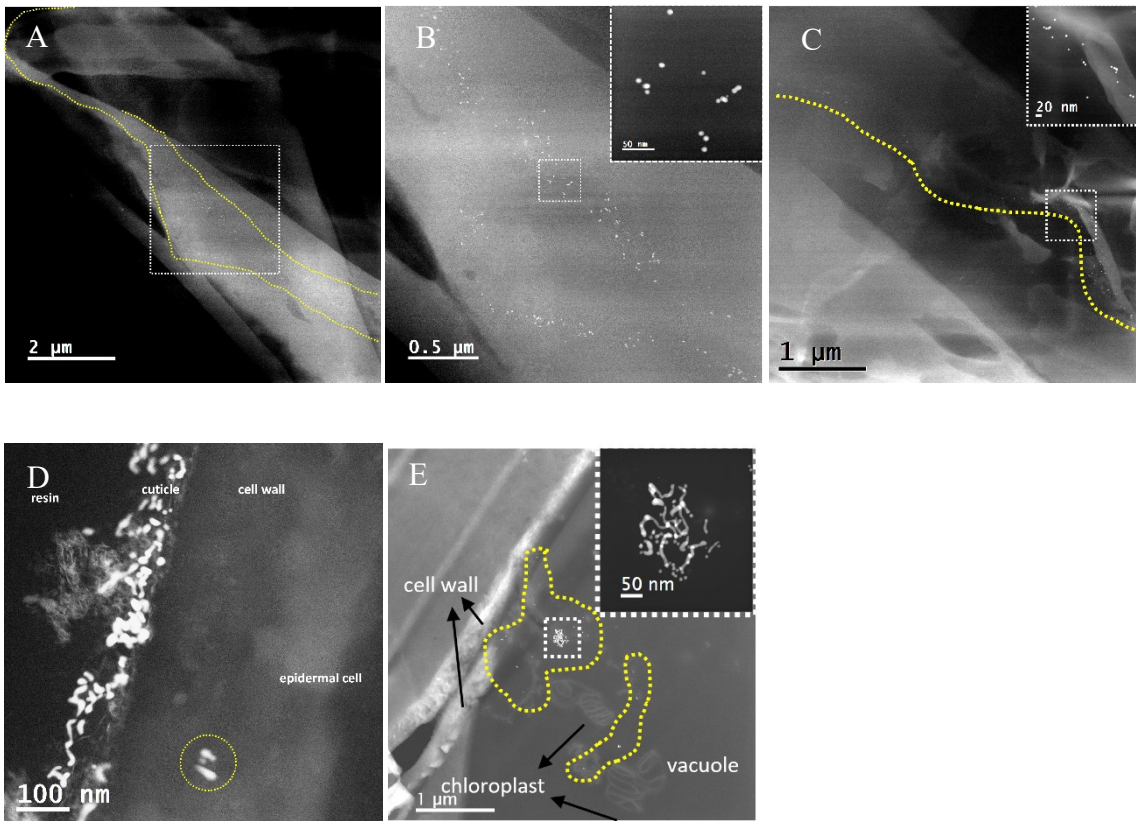


**Fig. S7** Additional HAADF-STEM images of Au nanocarriers translocating via a “highway” in plant leaves. (A-B) Spherical nanocarriers translocating in the cell wall. The white dotted box in (A) is magnified in (B). (C) shows another location containing Au spherical nanocarriers among cells. (D-E) show a location containing Au wire nanocarriers penetrating the cell wall and wire nanocarriers inside the cell. These results show the “highway” of nanocarriers translocation via apoplastic path.

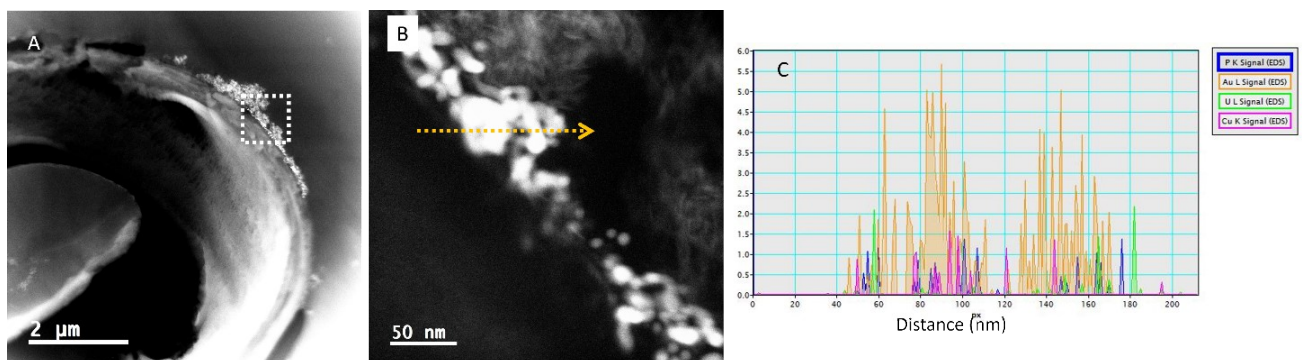


**Fig. S8** (A-B) Additional HAADF-STEM images of Au wire nanocarriers in plant leaf tissue and (C) an EDX line scan across the wire nanocarrier clusters at the plant-resin interface.

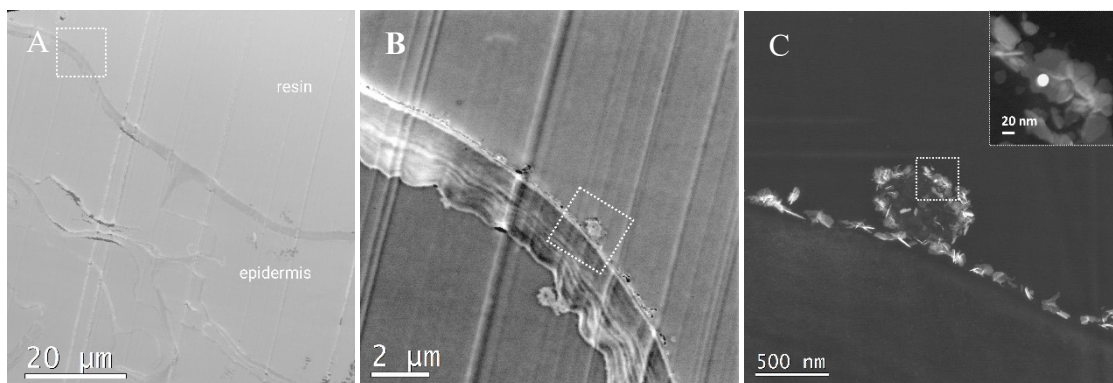


**Fig. S9** (A-C) Additional HAADF-STEM images of Au wire nanocarriers in the plant stem. The white dotted boxes in (A-B) are magnified in (B-C) to show areas containing nanocarriers. The inset dotted box in (C) shows a region containing a nanocarrier which is mostly re-deposited out the epidermis of plant stem.

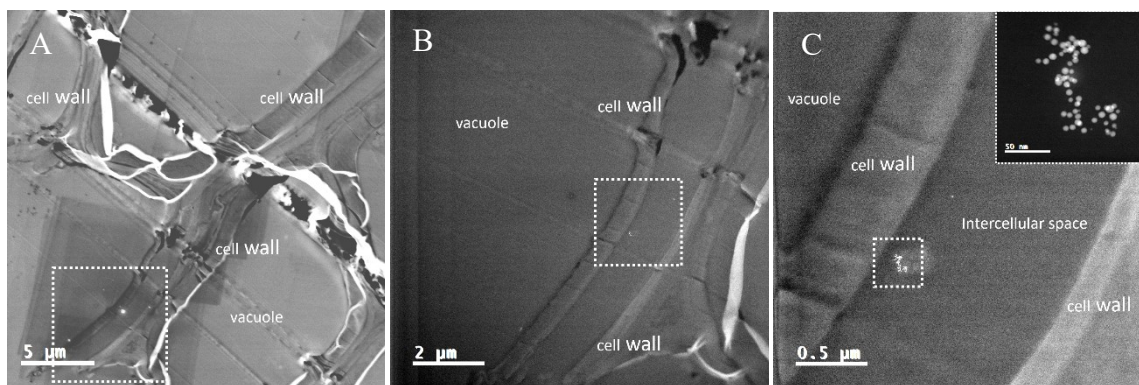


**Fig. S10** (A-C) Additional HAADF-STEM images of Au wire nanocarriers showing the storage of nanocarriers in the intercellular space in the plant root. The white dotted boxes in (A-B) are magnified in (B-C) to show the location of the nanocarriers. The inset dotted box in (C) shows a region containing a nanocarrier which is mostly stored in the plant root.

### 3. References

1. H. Rachmawati, C. A. Edityaningrum and R. Mauludin, Molecular inclusion complex of curcumin- $\beta$ -cyclodextrin nanoparticle to enhance curcumin skin permeability from hydrophilic matrix gel, *AAPS PharmSciTech*, 2013, **14**, 1303–1312.
2. Z. Zou, Z. Shi and L. Deng, Highly efficient removal of Cu(II) from aqueous solution using a novel magnetic EDTA functionalized  $\text{CoFe}_2\text{O}_4$ , *RSC Adv.*, 2017, **7**, 5195–5205.

3. M. Raoov, S. Mohamad and M. R. Abas, Synthesis and characterization of  $\beta$ -cyclodextrin functionalized ionic liquid polymer as a macroporous material for the removal of phenols and As(V), *Int. J. Mol. Sci.*, 2014, **15**, 100–119.
4. Y. S., M.-A. Pestovsky and Agustino, Synthesis of gold nanoparticles by tetrachloroaurate reduction with cyclodextrins, *Quím. Nova*, 2018, **41**, 926–932.
5. X. Ai, L. Niu, Y. Li, F. Yang and X. Su, A novel  $\beta$ -cyclodextrin-QDs optical biosensor for the determination of amantadine and its application in cell imaging, *Talanta*, 2012, **99**, 409–414.
6. B. Aswathy, G. S. Avadhani, S. Suji and G. Sony, Synthesis of  $\beta$ -cyclodextrin functionalized gold nanoparticles for the selective detection of Pb<sup>2+</sup> ions from aqueous solution, *Front. Mater. Sci.*, 2012, **6**, 168–175.
7. A. Alsaiee, B. J. Smith, L. Xiao, Y. Ling, D. E. Helbling and W. R. Dichtel, Rapid removal of organic micropollutants from water by a porous  $\beta$ -cyclodextrin polymer, *Nature*, 2016, **529**, 190-194.
8. V. Ramalakshmi and J. Balavijayalakshmi, Influence of gold nanoparticle concentration on polymer functionalized reduced graphene nanosheets and its electrochemical sensing performance, *Mater. Res. Express*, 2019, **6**, 075013.
9. R. H. A. Ras, J. Németh, C. T. Johnston, I. Dékány and R. A. Schoonheydt, Orientation and conformation of octadecyl rhodamine B in hybrid Langmuir–Blodgett monolayers containing clay minerals, *Phys. Chem. Chem. Phys.*, 2004, **6**, 5347–5352.
10. S. S. Ramos, A. F. Vilhena, L. Santos and P. Almeida, <sup>1</sup>H and <sup>13</sup>C NMR spectra of commercial rhodamine ester derivatives, *Magn. Reson. Chem.*, 2000, **38**, 475–478.
11. C. L. Phillips, T. Z. Regier and D. Peak, Aqueous Cu(II)–organic complexation studied in situ using soft X-ray and vibrational spectroscopies, *Environ. Sci. Technol.*, 2013, **47**, 14290–14297.
12. D. T. Sawyer and P. J. Paulsen, Properties and infrared spectra of ethylenediaminetetraacetic acid complexes. II. Chelates of divalent ions, *J. Am. Chem. Soc.*, 1959, **81**, 816–820.
13. R. Padmakumari, V. Ravindrachary, B. K. Mahantesha, R. N. Sagar, R. Sahanakumari and R. F. Bhajantri, Modification of fluorescence and optical properties of rhodamine B dye doped PVA/chitosan polymer blend films, *AIP Conf. Proc.*, 2018, **1953**, 030248.
14. Y. Huang, D. Li and J. Li,  $\beta$ -Cyclodextrin controlled assembling nanostructures from gold nanoparticles to gold nanowires, *Chem. Phys. Lett.*, 2004, **389**, 14–18.